

A WIDE-ANGLE MAGNETIC LENS FOR COLLECTING LOW-ENERGY π -MESONS IN A SOLID ANGLE OF 10 sr

G. I. SIL'VESTROV and V. A. TAYURSKY

Institute of Nuclear Physics, Novosibirsk 90, USSR

Received 14 September 1977

Optical characteristics and construction of a focusing device for collecting low-energy π -mesons in a solid angle of about 4π sr are considered. The focusing device is an axially-symmetric magnetic lens with magnetic field of ≈ 100 kOe and pulsating current of ≈ 1.4 MA. Parameters of a supply system operating at several hertz rate are given.

At area of 100 cm^2 in the focus plane of the system the $30\text{ MeV } \pi^-$ -meson flux, produced by 1 GeV electron beam, is $\approx 10^{-5}$ /electron with a maximum density of $3 \times 10^{-7} \pi^-/\text{cm}^2$.

1. Introduction

A production of intensive low-energy pion and muon beams is an actual problem for nuclear physics researches (see, for example, ref. 1), a mesochemistry²⁾ and a π -meson radiotherapy³⁻⁵⁾. For the pion production 600 – 800 MeV proton accelerators, having large currents (up to 6×10^{15} protons/s⁶⁾), are presently used. However, practically isotropically produced low-energy pions are being collected in a small solid angle. Therefore the question about an increase of pion-beams intensities, except an obvious way, an increase of proton currents, reduces to designing of focusing devices with maximum acceptance angles. There are several types of wide-angle focusing devices that, unlike traditional optical systems with quadrupoles for paraxial beams, enlarge an acceptance angle up to approximately one steradian. Such systems are divided into two classes: the solenoidal lenses with an uniform and a non-uniform magnetic field at the axis⁴⁾ and the iron⁷⁾ and non-iron⁸⁾ toroidal lenses. Magnetic fields in such lenses are being excited by direct currents and this fields are less than 20 kOe . Further increase of an acceptance angle is limited by two reasons. The first one is the spherical aberrations for the solenoidal lenses or the fringe effects because of scattered fields between current windings for the toroidal lenses. The second reason is an abrupt increase of lenses sizes and, consequently, a power consumption.

For beams with several hertz repetition rate it's possible to use the impulsive parabolic type lenses^{9,10)}. These have not mentioned before restrictions. The fringe effects are absent for the field is exactly restricted by the thinwalled current surfaces, through which particles pass and changing the form of which it's possible to remove the

spherical aberrations for any acceptance angle¹¹⁾. Moreover, the field amplitude in a pulsating regime can be enlarged to quantities more than 100 kOe ¹²⁾, that decreases the dimensions of the system and the power consumption.

The subject of the paper is a design of this type lens with an acceptance angle of about 10 sr . The efficiency of application of such systems for an intensive pion beams production by $\approx 1\text{ GeV}$ electron or proton beams is considered.

2. Focusing device

A possibility of the wide-angle focusing is obvious from the following consideration. Consider a point source with an isotropic angular distribution of particles on the axis of a thin-walled cylinder, through the walls of which leaks an electric current. This cylinder is an entrance surface. All particles with angles $0^\circ < \alpha < 180^\circ$ will cross the walls and move in an axially-symmetric magnetic field ($B \propto 1/r$). If we give for an exit surface, limiting the field, the shape, that all trajectories crossing it

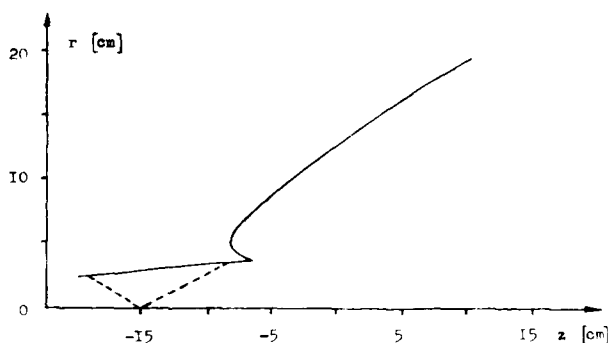


Fig. 1. The profile (one half) of the lens, that collects the beam with momentum $P = 100\text{ MeV}/c$, emitted from $z = -15\text{ cm}$, and converges it in $z = 50\text{ cm}$. For this profile all computations were carried out.

have the zero angle with the axis, we shall receive the focusing device, collecting practically all particles in a parallel beam. Changing the shape of the exit surface, one can receive the beam, that converges in a given point on the axis of the system. Fig. 1 gives the profile of the lens for which the focusing properties were studied. For decreasing of mechanical stresses in the place, where the cylindrical surface goes into the exit surface, the entrance surface was chosen to have the conic form. Its profile in r, z coordinates is given by the equation:

$$r = 0.1z + 4.2. \quad (1)$$

The exit surface was determined from the condition of hit of particles with momentum $P = 100 \text{ MeV}/c$ in the point $z = 50 \text{ cm}$. The source was placed in the point $z = -15 \text{ cm}$. The exit surface was calculated by means of numerical integration of equations of motion of particles in an axially-symmetric magnetic field:

$$B = B_0 \frac{r_0}{r}, \quad (2)$$

where B_0 is the field strength at the surface of radius r_0 . The lens collects the particles with angles $30^\circ < \alpha < 150^\circ$. The convergence angle in the focus of the system is $\alpha_{\text{conv}} \approx 25^\circ$. The maximum trajectory radius for $\alpha = 150^\circ$ is $r_{\text{max}} = 22 \text{ cm}$. For a pulsating current amplitude of 1.4 MA , a maximum field at the entrance surface at $r = 2.5 \text{ cm}$ is $B_{\text{max}} = 112 \text{ kOe}$. In this focusing device the spherical aberrations are absent, but appears an additional size of the beam in the focal plane because of scattering in the walls. The last can be neglected, if it is small compared with the size, that is due to a non-point likeness of the source. In calculations of the scattering effects in the lens the entrance surface was taken of 0.5 cm thickness and the exit surface of 0.2 cm thickness. The walls were assumed to be made out of aluminium, that bears the maximum strains of $2000 \text{ kg}/\text{cm}^2$. The scattering was calculated according to the Molière theory. With the mentioned parameters and the point-like source (placed in the point $z = -15 \text{ cm}$) the average square of the beam radius in the focal plane ($z = 50 \text{ cm}$), connected with the scattering in the walls, is equal to $\langle R_\theta^2 \rangle = (23 \pm 1.7) \text{ cm}^2$. The scattering in the entrance surface gives: $\langle R_{\theta_1}^2 \rangle = (18 \pm 1.4) \text{ cm}^2$ and in the exit surface $\langle R_{\theta_2}^2 \rangle = 6.6 \pm 0.6 \text{ cm}^2$. The curve in fig. 2 shows the average square of the beam radius in the focal plane for the source of $L \text{ cm}$ length without the

scattering of particles in the walls. It was assumed that particles are uniformly produced along the target axis. This quantity is being compared with $\langle R_\theta^2 \rangle$. One can see, that for the target of more than $L_\theta \approx 2.1 \text{ cm}$ length, $\langle R_L^2 \rangle > \langle R_\theta^2 \rangle$. Thus the scattering can be neglected for the target of $L \geq L_\theta$ length.

The lens does not collect the particles going forward in a solid angle of about 1 sr . There is placed a tungsten cone stopper. This stopper restricts the drift space outside the exit surface (fig. 3). For trajectories with a big radius, the drift space is limited by the walls of a cone hole in the shield. That is, the space between this cone surfaces serves as a diaphragm for a pion beam and restricts a momentum spectrum of particles passing across the lens (fig. 5). To separate a beam better one can place inside the lens several additional cone diaphragms along the trajectories of equilibrium particles.

3. Construction of the lens and a supply system

The experience of designing and investigation of the thin-walled covers with a big pulsating current^{9,10,12}) shows, that the covers conserve the mechanical firmness at more than 100 kOe magnetic field. A specific form of the current surfaces profiles of the described lens needs a special investigation of its mechanical properties in the regime of the dynamical loading, but this question is not discussed in the paper. The major problem in elab-

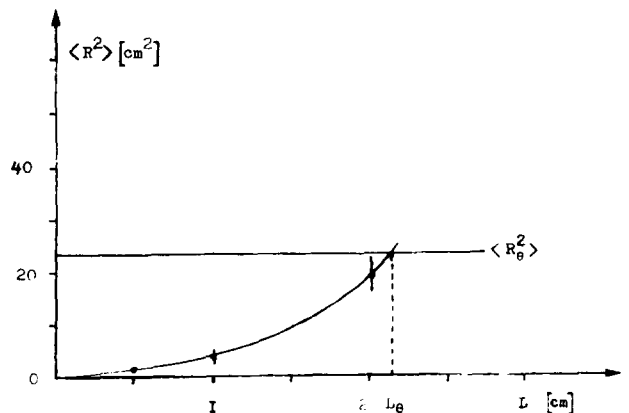


Fig. 2. The comparison of the beam size in the focal plane for the point-like source, taking account of pion scattering in the walls of the lens, with the beam size for the elonged source, but without scattering in the walls. The center of the converter is placed in the point $z = -15 \text{ cm}$. It was assumed, that particles of momentum $P_\pi = 100 \text{ MeV}/c$ emerge uniformly along the converter axis.

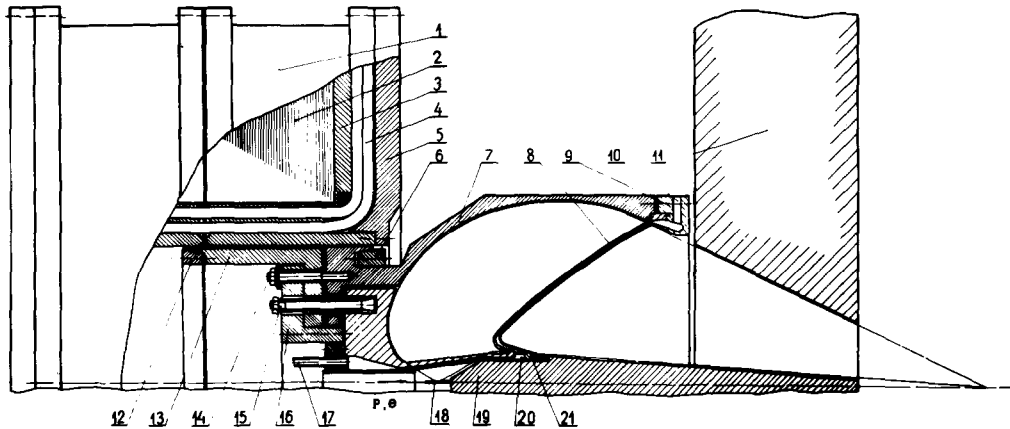


Fig. 3. The complete view of the focusing device. 1 - transformer; 2 - toroidal iron; 3 - secondary coil winding of the transformer; 4 - primary coil windings; 5 - cover; 6, 12 - pressing rings of the grip contacts; 7 - profilled coaxial tyre; 8 - body of the lens; 9 - pressing contact ring; 10, 17 - entrance and exit of the colling system; 11 - lead shield; 13 - coaxial current contacts; 14 - load-bearing bolts, supporting the tyre; 15 - contact grips; 16 - stop flange for supporting the pressing and pressing out bolts; 18 - converter target; 19 - tungsten stopper; 20 - stop passage detail; 21 - corpus of the water cooling.

orating of the lens is a construction of electrical contacts for currents up to 1.4 MA. For rigidly done up ends of the lens and for necessary contact efforts the electrical contacts must not give additional static strains in cross-sections of the lens. Another important problem is a creation of an intensive cooling of the thin-walled current surfaces, operating at several Hertz rate. Fig. 3 gives the lens with contact buses and a transformer. The lens is inserted in the profilled along the external trajectory coaxial tyre (7); the pressing ring (9) reinforces the lens at its end. The second end of the lens is not rigidly reinforced in the longitudinal direction and it's connected with the electrical contact (13) with the help of 18 grip dumes (15), uniformly distributed along the perimeter of the end. After dighting the contacts, the free end of the lens is firmly fixed relative to the detail (16) with the help of a system of the alternating pressing and pressing out bolts. The cone-like tungsten stopper (19), serving for absorption of particles after the target, is a load-bearing element of the construction in the same time. Through the passage detail (20), the stopper is pressed to the body of the lens at the place, where the entrance and exit surfaces join together. This place is the third point of support of the lens.

There are two variants of a water cooling of the lens. At cycles rate ≈ 0.2 Hz and less, the power, emitted in the lens, can be dissipated by a pulverization of water at its internal surface¹²). In fig. 3 the more intensive cooling system is represented.

In this case we lose a little in transparency, but such cooling system can provide a better dissipation of heat. This cooling system can dissipate about 100 W/cm^2 from the cone part of the lens and operate at several hertz current pulses repetition frequency. For this purpose the body of the lens is done out of two layers. This permits to create better conditions for the dissipation of heat with the help of a continuous stream of water between the layers. The internal non-current surface of the lens is done out of two parts. The parts are hermitized at the ends at the place of contact with the stopper, as it is shown in fig. 3.

The lens is supplied by the unipolar puls of sinusoidal current formed by the discharge of a capacity battery on the lens, that represents an inductive load. The capacity battery is switched on with the help of a thyristor valves system and discharges on the lens through the matching transformer having a small dissipation. The technique of creation of such generators is well developed at present¹⁴). The lens has an inductance of 50 nH and at a current of 1.4 MA the magnetic field energy in the operating volume is about 50 kJ. For a pulse duration of $100 \mu\text{s}$ the voltage on the lens is equal to 2.5 kV and for a transformation ratio of 10, it is necessary to commutate in the primary coil a current of 140 kA at a voltage of $V_1 = \pm 15 \text{ kV}$. This voltage is calculated taking account of parasitic parameters of the transformer. The transformer has the grounded center point. A reactive power of the transformer is equal to

4 GW. This generator has been constructed in IYaF SO AN and it is being tested at present. Diminishing a current frequency one can scale up a pulse duration. In this case the generator simplifies considerably. A Q -factor of the lens is high enough ($Q \approx 50$). The active power losses in the contour at 10 Hz frequency are equal to 15–20 kW. In this case the maximum heat flux in the cone part of the lens is about 100 W/cm².

4. Parameters of π^- -meson beam

Creation of focusing devices, collecting practically all π -mesons of a given momentum interval, produced in a target, will permit to have intensive meson beams not only from proton accelerators, but also from electron accelerators. First this question was discussed in ref. 5. From this work follows, that a pion flux in a focus of a special system will be only 30 times less for the electron conversion in comparison with the proton conversion at about 1 GeV energy and for the same collection conditions.

For the focusing system that we consider, geometrical conditions of the pion production are different for the proton and electron conversions. For an effective use of the proton beam the converter target should be about one inelastic nuclear interaction length long ($\lambda_{in} \approx 10$ cm for tungsten at $E_p \approx 1$ GeV). For the electron beam the target should be 2–3 times as long as $t_{max}(E_\gamma > m_\pi)$, where $t_{max} \approx 1.5 X_0$ (¹⁶) is the maximum position of the shower curve for photons of energy $E_\gamma > m_\pi$ (m_π -pion mass) at $E_e = 1$ GeV. For tungsten the radiation length is $X_0 = 0.35$ cm. In the last case the pion source is more "bright". This slightly compensates a relatively low conversion efficiency for the electron beam.

In the given below calculations of the conversion efficiency for the electron beam we use the cylindrical tungsten target of $L = 2$ cm length ($5.7 X_0$ of Wo). For this target the beam size in the focal plane given by dispersion of pion production points is equal to the dimension because of scattering in the walls of the lens (fig. 2). It was assumed for simplicity that pions emerge uniformly along the target axis. Really most pions emerge in the area of t_{max} , so the calculations make a picture worse, and the beam size in the focal plane will be determined mostly by the scattering in the walls. The incident beam was assumed to be infinitely thin and we neglected by the ionisation losses and multiple scattering of pions in the target.

For the incident beam energy of $E_e \lesssim 1$ GeV the main input in a π^- -yield from the target gives a single photoproduction of pions from the target nuclei by γ -quanta of the electron-photon shower in the converter. To estimate the π^- -momentum spectrum we used the experimental data on the pion photoproduction from carbon and copper nuclei^{17,18}). From ref. 18 follows that for the photon energy: $300 \lesssim E_\gamma \lesssim 700$ MeV and $\theta_{lab} \approx 28^\circ$ the cross-section depends on $A-Z$ as:

$$\frac{d\sigma}{d\Omega} \propto (A-Z)^{0.8}, \tag{3}$$

where A - atomic weight, Z - atomic number. From the data on the π^- photoproduction from neutrons¹⁹) follows, that at $E_\gamma \lesssim 1$ GeV the low-energy pions emerge almost isotropically in the laboratory system ($d\sigma/d\Omega \approx \text{const}$). Using this data we have for the π^- -yield from the target the following expression:

$$\frac{dN_\pi}{d\rho_\pi} = \frac{N_A}{A} \left(\frac{A-Z}{6} \right)^{0.8} \int_{E_{thr}}^{E_e} g(E_e, E_\gamma) dE_\gamma \int_0^\pi 2\pi \times \\ \times \sin \alpha d\alpha \frac{d^2 \sigma_c(E_\gamma, P_\pi, \alpha)}{dP_\pi d\Omega}, \tag{4}$$

where P_π - the momentum and E_π - the energy of pions, $E_{thr} \approx E_\pi$ - the threshold energy for the pion photoproduction, $g(E_e, E_\gamma) = 0.57 X_0 E_e/E_\gamma^2$ - the differential track length of photons^{20,21}), E_e - the incident electron beam energy, E_γ - the photon energy, N_A - the Avogadro number, $d^2 \sigma_c(E_\gamma, P_\pi, \alpha)/dP_\pi d\Omega$ - the twice differential single π^- -mesons photoproduction cross-section from carbon nuclei^{17,18}). A numerical integration of eq. (4) gives dN_π/dP_π in fig. 4. From this figure

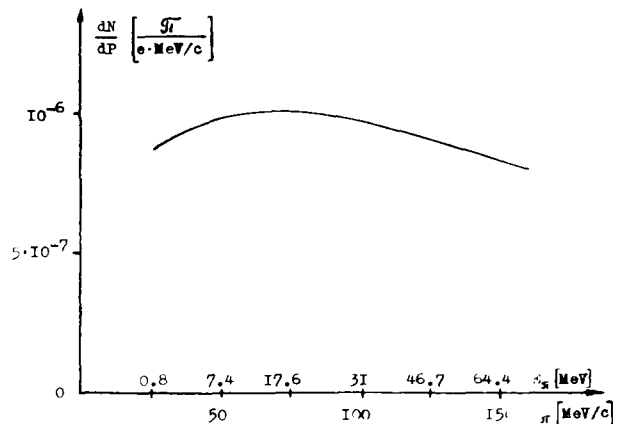


Fig. 4. The spectrum of the pions, produced in the tungsten converter by 1 GeV electrons.

follows that the spectrum does not change appreciably for $P_\pi = 100\text{--}150$ MeV/c and one can use for estimates:

$$\frac{dN_\pi}{dP_\pi} \approx 10^{-6} \pi^- \text{ MeV}^{-1} \text{ c (incident electron)}^{-1}. \quad (5)$$

The momentum spectra of π^- -mesons in the focal plane of the lens are represented in fig. 5. The histograms give pion spectra within circles of different radii R (1 - $R = 2$ cm, 2 - $R = 4$ cm, 3 - $R = 8$ cm). The spectra are normalized to the total numbers of pions produced with angles $30^\circ < \alpha < 150^\circ$ in the 5 MeV/c momentum intervals. Their maxima moved from $P_\pi = 100$ MeV/c, for which the profile of the lens was computed, to $P_\pi = 105\text{--}110$ MeV/c. This shift is due to the scattering in the entrance surface of the lens. The scattering causes decreasing of the transverse in respect to the field momentum component, which is responsible for the focusing. The average density of π^- -meson flux within a circle of radius R per incident electron, as well as the expected flux densities of e^- , μ^- , n contamination, is adduced in table 1.

The estimate of the μ^- contamination from $\mu^- - \mu^+$ pairs was done according to ref. 22.

The neutron contamination accounting the at-

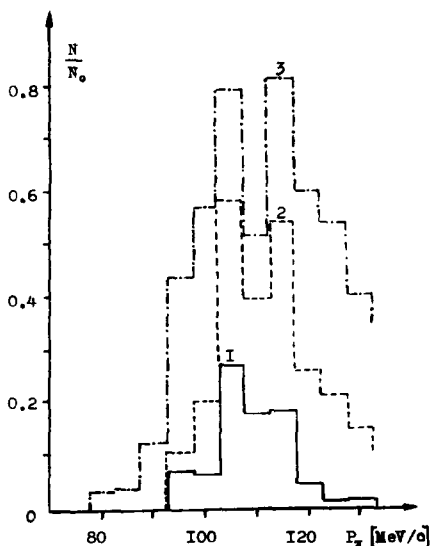


Fig. 5. The momentum spectrum of the pions in the focal plane. It was assumed, that pions emerge uniformly along the axis of 2 cm converter. The center of the converter is placed in $z = -15$ cm. The multiple scattering of π^- in the walls is taken into consideration. 1 - the spectrum within a circle of 2 cm radius; 2 - the same for the circle of 4 cm radius; 3 - the same for the circle of 8 cm radius.

TABLE 1

 Particle flux densities (part./cm²)

Particle	$R=2$ (cm)	4 (cm)	8 (cm)	Momentum interval (MeV/c)
π^-	3×10^{-7}	1.7×10^{-7}	7×10^{-8}	105 ± 15
e^-	6×10^{-6}	3.4×10^{-6}	1.4×10^{-6}	105 ± 15
μ^-	3×10^{-10}	1.7×10^{-10}	7×10^{-11}	105 ± 15
n	3×10^{-8}	3×10^{-8}	3×10^{-8}	-

tenuation of particles in the tungsten stopper, was estimated according to ref. 23.

The flux of electrons, leaving the converter, was computed with the help of the program in ref. 24. The major input in the electron contamination goes from the tails of angular distribution of electrons with $P = 100$ MeV/c in the converter target. This contamination can be diminished by the increase of the angle occupied by the stopper. Some estimates show, that for the angle of 40° the contamination diminishes by a factor of 4.

For a comparison with this calculations, there were performed some estimates of the conversion efficiency for the proton beam of energy $E_p = 730$ MeV. A tungsten target of 10 cm length was used in calculations. The center of target was placed in the point $z = -15$ cm. The points of emission of pions were sampled from the distribution $f(z) \propto \exp(-z/\lambda_{in})$. To evaluate the pion yield from tungsten nuclei we used the experimental data¹⁵⁾ at 730 MeV proton energy (from lead nuclei). An extrapolation of this data to $P_\pi = 100$ MeV/c gives:

$$\frac{dN_\pi}{dP_\pi} \approx 10^{-4} \pi^- \text{ MeV}^{-1} \text{ c} \quad (6)$$

per inelastic interaction. The average density of π^- -meson flux within a circle of radius R per incident proton in the focal plane of the system is given in table 2.

TABLE 2

 Pion flux density (pions/cm²)

Particle	$R=2$ (cm)	4 (cm)	8 (cm)	Momentum interval (MeV/c)
π^-	3×10^{-5}	1.5×10^{-5}	7.5×10^{-6}	105 ± 25

It should be noted that in this case the momentum spectrum of pions is more wide than for the electron conversion. This is connected with the chromatic properties of the lens for extended sources.

In the case of the proton conversion an operation with the pion beam in the focus of the system will be difficult, apparently, because of very high proton and neutron fluxes. A local shield after the converter is not enough in this case, so it will be necessary to have a special channel to transport the meson beam in an area with the better radiation conditions.

5. Conclusions

The principal and technical possibility of creation of the focusing device, that can collect practically all low-energy pions produced in the converter, was shown in the paper. The described construction is a sketch project of one possible variant of such systems. We considered the limit parameters of the system (a field, a current, a heat loading). This parameters can be optimized and diminished for the concrete constructions. We have given the detailed description of some technical details of the focusing device to show, that the modern development of the strong pulsating magnetic fields technique ($B > 100$ kOe) and the large pulsating currents technique ($I > 1$ MA) allows to choose the parameters of such systems in the indicated range of fields and currents without any fear of the principal technical difficulties.

Unlike the considered system, the presently existing wide-angle focusing devices with the static magnetic fields^{4,5,7}) have two obvious failures: (a) a small in comparison with 4π acceptance angle, (b) large longitudinal dimensions, so that the particle trajectory lengths are about the decay length for low-energy pions. Creation of systems with the large pulsating magnetic fields will allow to enlarge the acceptance angle by a factor of 10–20 and to decrease the lengths of trajectories up to about 1 m, that practically excludes the pion decay. This will allow to increase the conversion efficiency almost by a factor of 100. Especially attractive seems to be the possibility of production of sufficiently intensive meson beams at electron accelerators of 1 GeV or more energy, because of their lower cost and because of the lower activation of the electrical and physical equipment under the electron beams.

The authors are much indebted to valuable discussions with acad. A. N. Skrinsky, drs. T. A. Vsevolozskaya, V. I. Kupchik, V. I. Karasyuk, G.I. Villewald, V. I. Zaicev, A. D. Chernyakin and B. Ya. Chudaev.

References

- 1) V. P. Dzelepov, V. P. Dmitrievsky and V. V. Col'ga, in *Problemy Yadernoy Fiziki i Fiziki Elementarnykh Chastits (Problems of nuclear physics and physics of elementary particles)* (Nauka, Moscow, 1975) in Russian.
- 2) V. I. Gol'dansky, *Trudy III Vsesoyuznogo Soveshaniya po Uskoritelyam (Proceedings of the III Soviet Particle Accelerators conference)* vol. I (1973) p. 62, in Russian.
- 3) N. N. Blochin, *Ibid.*, 43.
- 4) V. M. Abazov, B. P. Dzelepov, E. S. Kuz'min, G. A. Molokanov, O. V. Savchenko, G. P. Reshetnikov and E. P. Cherevatenko, *Preprint OIYaI P13-879*, in Russian.
- 5) *Particle Accelerators* 5 (1975) 57.
- 6) R. L. Burman, R. L. Fulton and M. Yakobson, *Nucl. Instr. and Meth.* 131 (1975) 29.
- 7) P. Kofoed-Hansen, J. Lindhard and O. B. Nielsen, *Det. Kgl. Danske Vidensk. Sels. Kab., Math-Fys. Medd.* 16 (1950) 25.
- 8) V. V. Vladimirovsky, E. K. Tarasov and Yu. V. Trebuchovskiy, *Pribory i Technika Eksperimenta (Soviet Journal on Installations and Technique of Experiment)* N 1 (1956) 13, in Russian.
- 9) L. L. Danilov, S. N. Rodionov and G. I. Sil'vestrov, *Jurnal Technicheskoy Fiziki (Soviet Journal of Technical Physics)* 37 (1967) 914, in Russian.
- 10) T. A. Vsevolozskaya, L. L. Danilov, V. N. Karasyuk and G. I. Sil'vestrov, *Trudy II Vsesoyuznogo soveshaniya po uskoritelyam*, vol. II (1972) 224, in Russian.
- 11) T. A. Vsevolozskaya and G. I. Sil'vestrov, *Jurnal Technicheskoy Fiziki* 43 (1973) 61, in Russian.
- 12) G. S. Villewald, V. N. Karasyuk and G. I. Sil'vestrov, *Preprint IYaF SOAN 75-98*, in Russian.
- 13) D. G. Baratov, V. M. Valov, R. A. Rzaev, B. L. Rykov and I. M. Shalashov, *Prikladnaya Mekhanika i Technicheskaya Fizika (Soviet Journal of Applied Mechanics and Technical Physics)*, N 3 (1974) 133, in Russian.
- 14) B. F. Baratov, A. V. Iljin, V. M. Pakin and G. I. Sil'vestrov, *Trudy I Vsesoyuznogo soveshaniya po uskoritelyam* 1 (1969) 283, in Russian.
- 15) D. F. R. Cohran, P. N. Dean, P. A. Gram, E. A. Knapp, E. R. Martin, D. E. Nagle, R. B. Perkins, W. Y. Schlaer, H. A. Thiessen and E. D. Theriot, *Phys. Rev. D* 6 (1972) 3085.
- 16) H. Nagel, *Zeits. für Phys.* 186 (1965) 319.
- 17) I. Endo, K. Baba, H. Fujii, Y. Sumi, S. Anami, S. Ninomiya, S. Kato and A. Marakami, *Phys. Lett.* 47B (1973) 469.
- 18) Y. Sumi, in *Proc. INS Symposium on Electron and photon interactions at resonance region and related topics*, Tokio (1975) p. 185.
- 19) H. H. Fisher, in *Proc. of the 6th International Symposium on Electron and photon interactions at high energies*, (1975) p. 75.
- 20) B. Rossi, *High energy particles* (Prentice-Hall, Inc. Englewood Cliffs, New Jersey, 1952).

- 21) C. D. Zerby and M. S. Moran, *J. Appl. Phys.* **34** (1965) 2445.
- 22) W. R. Nelson, *Nucl. Instr. and Meth.* **66** (1968) 293.
- 23) V. P. Prichod'ko and V. Ya. Chudayev, Preprint IYaF SOAN 74-35, in Russian.
- 24) F. M. Izraelev, V. S. Synach, V. A. Tayursky, B. V. Chirikov and V. V. Shmakov, Preprint IYaF SOAN 63-73, in Russian.